

Article

Covalent Porphyrin Hybrids Linked with Dipyrin, Bidipyrin or Thiacorrole

Renbao He, Huan Yue and Jiahui Kong * 

Zhejiang Yongtai Technology Co. Ltd., Taizhou 317016, China; Renb755701@163.com (R.H.); helenyue668@163.com (H.Y.)

* Correspondence: kongjia159@163.com; Tel.: +86-188-1823-8137

Received: 3 August 2017; Accepted: 20 August 2017; Published: 23 August 2017

Abstract: Novel meso-meso directly linked porphyrin hybrids were successfully targeted and synthesized, with porphyrin units linked with dipyrin, bidipyrin or thiacorrole, expanding the ranges of dipyrin derivatives and showing diverse metal coordinations and further influencing the chemical shift of pyrrole units. The porphyrinyl dipyrin nickel complex **3** was successfully obtained in a high yield by the oxidation of porphyrinyl dipyrromethane **2** and subsequent coordination. Further oxidative coupling reactions of **3** afforded por-bidipyrin-por hybrid **4**. Interestingly, an unexpected methoxy por-bidipyrin-por hybrid **6** was generated by treating **4** with FeCl₃ in CH₂Cl₂/MeOH and subsequent coordination. In addition to open chain hybrids, an aromatic scaffold hybrid por-thiacorrole-por **8** was synthesized by treating porphyrinyl dibromo-dipyrin nickel complex **7** with Na₂S·9H₂O. A series of porphyrin hybrids offers a new approach for π -conjugated molecules.

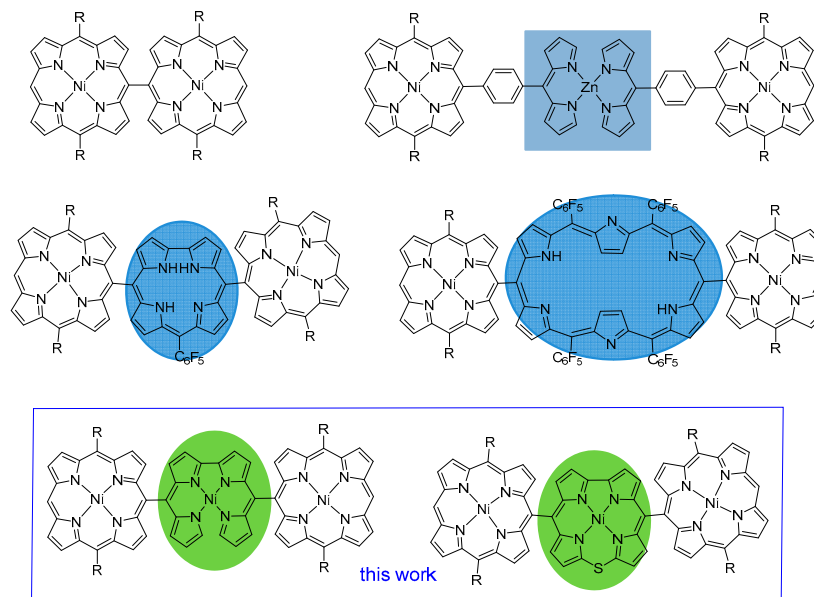
Keywords: porphyrin; hybrid; thiacorrole

1. Introduction

In recent years, molecules with highly extended π -conjugation have attracted much attention, owing to their excellent properties in organic semiconductor devices, near-infra-red (NIR) dyes and non-linear optical materials [1–4]. In this regard, dipyrin, containing conjugated pyrrole units, has been used extensively for synthesis of π -conjugated molecules and fluorescent or colorimetric ion probes [5–12]. Based on dipyrin, bidipyrin, which represents a class of bile pigments with two dipyrin units linked directly by α -carbons, further extends the π -conjugation, and has been extensively researched with regard to catalysis, magnetism and optics [13–16]. Moreover, covalently linked dipyrins or bidipyrins demonstrate a novel approach to obtaining more highly conjugated or more structurally interesting molecules [17–19].

On the other hand, porphyrin, a highly conjugated tetrapyrrolic compound, plays an important role in π -extended dyes [20–24]. Various porphyrin types have been explored, including two-dimensionally expanded porphyrin sheets, donor-acceptor type and electron-deficient type (Scheme 1) [25–29]. π -conjugated porphyrins contain multiple porphyrin units linked in various linking fashions, such as meso-meso, β - β , and β - β triply-linked methods [22,30–34]. Among these conjugated porphyrins, meso-meso linked porphyrin hybrids with a short center-to-center distance are extremely important, because they are favorable for achieving rapid energy-transfer [35,36]. Additionally, covalently linked multiporphyrin hybrids have different photodynamic and electrochemical properties depending on the type of linkages. For example, the Osuka group has successfully constructed meso-meso linked porphyrin arrays with excellent photophysical properties using a unique oxidation method [37]. Corrole, a ring contracted porphyrinoid, has one peripheral meso carbon less and one inner NH more, compared with porphyrin, which presents different properties for stabilizing higher

oxidation states of metals, and a different coordination chemistry. When corrole and porphyrin are linked by the meso-meso method, the hybrids demonstrate novel properties with higher quantum yield and longer life time [38,39]. Moreover, hexaphyrin, an expanded porphyrin type, shows a larger π -conjugation and intra-annular cavity. The meso-meso linked porphyrin-hexaphyrin-porphyrin hybrid revealed a distorted conformation and adopted a Möbius aromatic twisted structure for the [28- π] hexaphyrin moiety in solution [40,41].



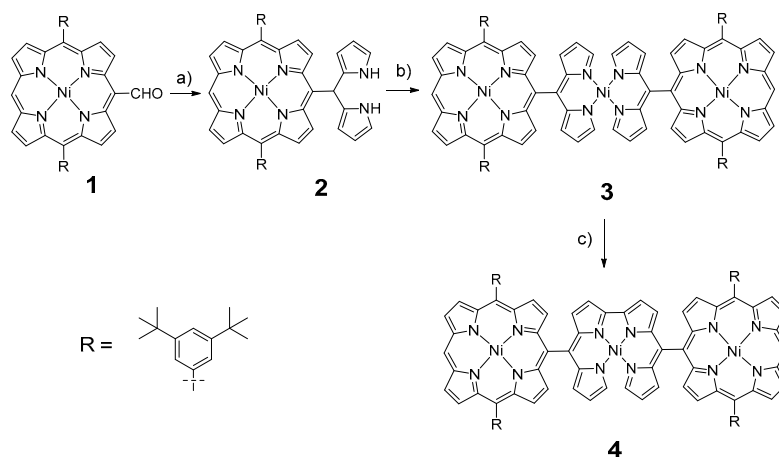
Scheme 1. Porphyrin dimer and hybrids linked in various fashions.

Furthermore, when porphyrin and dipyrin or bidipyrin are covalently linked, the new dyes simultaneously show the rigid and planar properties of porphyrin unit and the coordination and flexible properties of the dipyrin or bidipyrin unit [42,43]. On the other hand, apart from the above-mentioned hybrids, thiacorrole [44], a *meso*-modified porphyrin analogue with heteroatom directly on the π -conjugation circuit, could potentially be introduced into the porphyrin hybrids; this hybrid remains unexplored. The new hybrids could possibly present interesting coordination or magnetism properties related to different units. In spite of rich examples of porphyrin hybrids, to the best of our knowledge, the study of porphyrin dipyrin, bidipyrin or thiacorrole hybrids is still rare. Therefore, there is plenty of room for improvement in synthetic routes to the development of new porphyrin hybrids. Moreover, the new hybrids would demonstrate different metal distances and metal coordination environments, and the different environments would effectively influence properties of pyrrole units in the middle part of the hybrids. In the present work, we report the first synthesis of meso-meso directly linked por-dipyrin-por, por-bidipyrin-por and por-thiacor-por hybrids, and further investigate the spectroscopic properties of these hybrids.

2. Results and Discussion

A synthetic route for porphyrin-dipyrin-porphyrin (por-dipyrin-por) hybrid was achieved by following the method illustrated in Scheme 2. *meso*-Porphyrinyl dipyrromethane **2** was prepared by TFA-catalyzed condensation of *meso*-formylated Ni(II) porphyrin **1** with excess pyrrole in a 65% yield. After dipyrromethane **2** was oxidized with 2,3-dichloro-5,6-dicyano-1,4-benzoquinone (DDQ) in THF, and reacted with NiCl₂·6H₂O, the porphyrinyl dipyrin nickel complex (por-dipyrin-por) **3** was obtained in a good yield. The molecular mass of the triad, detected by HRMS, was fully consistent with calculated value: m/z [M + H]⁺ = 1825.7453 (calcd. for 1825.7428). The ¹H-NMR spectrum of **3** in CDCl₃ revealed that as the result of the electron withdrawing and paramagnetism effect of nickel

metal and deshielding influences of aromatic circulation of the two near porphyrin cycle, the broad signals for four pyrrolic α -CHs and pyrrolic β -CHs in dipyrryn units were downfielded and observed at 13.96 ppm and 9.89 ppm, respectively (Figure 1). Because of the effect of nickel metal, the remaining α positions of pyrroles become more reactive, and could potentially be oxidized to form a new C-C bond. Consistent with this, when complex **3** was reacted with DDQ in reflux toluene, the dipyrryn units were successfully linked with a new C-C bond to afford a novel por-bidipyrryn-por hybrid **4** in a 59% yield. HRMS of **4** lied in m/z $[M + H]^+ = 1823.7160$, which is consistent with calcd. result (calcd. for 1823.7272). The $^1\text{H-NMR}$ spectrum of **4** in CDCl_3 confirmed the structure with the disappearance of the downfield broad signal at 13.96 ppm, and the pyrroles CHs appeared at 5.9–6.7 ppm. It is worth noting that, compared with hybrid **3**, the α -CHs of **4** was significantly upfielded owing to the C-C bond, which is consistent with the reported results [13–16]. More solid structural evidence for **3** and **4** came from the single crystal X-ray diffraction analyses (Figures 2 and 3), which revealed that the Ni^{II} ion of complex **3** is coordinated with two dipyrryn chelates in a pseudo-tetrahedral environment, as expected for such compound. However, the Ni^{II} ion adopted a distorted square planar environment for complex **4**, as the result of the repulsion between the two remaining α -CHs.



Scheme 2. Synthesis of porphyrin dipyrryn hybrid **3** and bidipyrryn hybrid **4**. Reaction conditions: (a) excess pyrrole, TFA; (b) DDQ, Et_3N , $\text{NiCl}_2 \cdot 6\text{H}_2\text{O}$, $\text{CH}_2\text{Cl}_2/\text{MeOH}$; (c) DDQ, toluene, reflux.

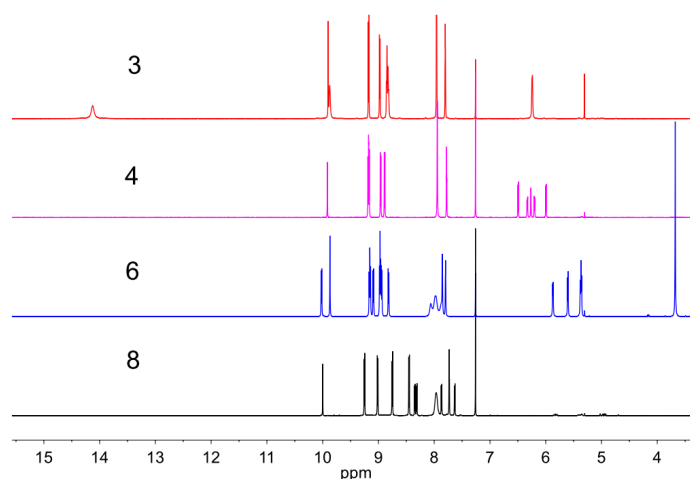


Figure 1. The aromatic regions $^1\text{H-NMR}$ of porphyrin hybrids **3**, **4**, **6** and **8**.

On the other hand, hybrid **4** demonstrates the porphyrin linked by an opened tetrapyrrolic complex. We wanted to explore the possibility to further synthesizing hybrids linked by macrocyclic frameworks. Considering that there are α positions remaining in **4**, it is possible to form further

conjugated frameworks, when exposed to some oxidants. Interestingly, when **4** was treated with FeCl_3 in $\text{CH}_2\text{Cl}_2/\text{MeOH}$, a new product (**5**) was detected (Scheme 3). Unfortunately, compound **5** was unstable. We used $\text{Ni}(\text{OAc})_2 \cdot 2\text{H}_2\text{O}$ to coordinate with **5** to afford complex **6**. The $^1\text{H-NMR}$ spectrum of **6** revealed that the signal of methoxy groups appeared at 3.69 ppm, indicating no expected ring-closure products. Compared with **4**, the β -CHs of the bidipyrrin unit in **6** were slightly upfielded, which may be ascribed to the electron-donating effect of the methoxy groups.

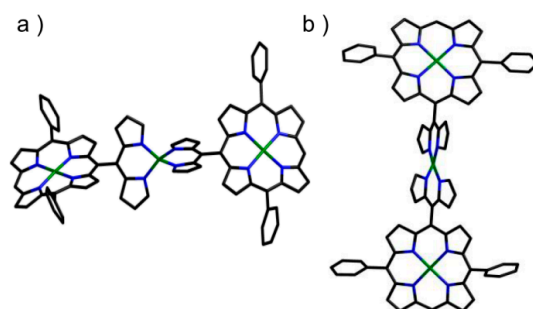
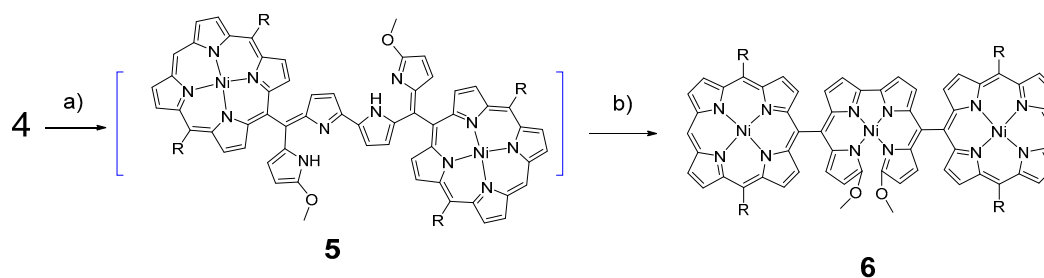
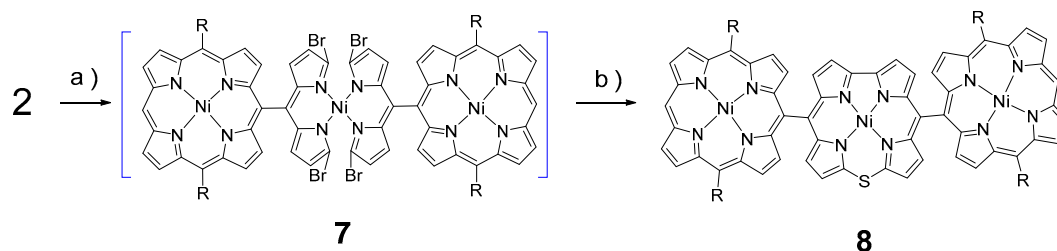


Figure 2. X-ray crystal structures of **3**. Solvent molecules, *tert*-butyl groups and hydrogen atoms were omitted for clarity (a) top view; (b) side view.



Scheme 3. Synthesis of substituted porphyrin bidipyrrin hybrid **6**. Reaction conditions: (a) FeCl_3 , $\text{CH}_2\text{Cl}_2/\text{MeOH}$; (b) $\text{Ni}(\text{OAc})_2 \cdot 2\text{H}_2\text{O}$, $\text{CH}_2\text{Cl}_2/\text{MeOH}$.

In addition to the open chain units, it is interesting to investigate porphyrin hybrids linked with aromatic scaffolds. The synthetic protocol of por-thiacorrole hybrids was illustrated in Scheme 4. Consecutive treatment of porphyrinyldipyrromethane **2** with NBS, DDQ and $\text{NiCl}_2 \cdot 6\text{H}_2\text{O}$ gave the bis(dibromodipyrrin)Ni(II) complex **7** in a high yield (by TLC). Unfortunately, complex **7** was unexpectedly unstable, and was able to be decomposed when exposed to the air. We found that the 10-thiacorrole **8** was obtained by treatment of complex **7** with sodium sulfide hydrate in DMF at 65°C in an excellent yield. The $^1\text{H-NMR}$ spectrum of hybrid **8** revealed that the β -CHs in porphyrin units lay in the range of 8.4–9.4 ppm, and the meso-CHs lay at 10.0 ppm, which is consistent with porphyrin properties. Interestingly, the β -CHs of the 10-thiacorrole unit lay in the range of 7.6–8.4 ppm, slightly downfielded compared with **4**, which is related to the aromatic scaffold.



Scheme 4. Synthesis of porphyrin thiacorrole hybrid **8**. Reaction conditions: (a) (i) NBS, -78°C ; (ii) DDQ; (iii) $\text{NiCl}_2 \cdot 6\text{H}_2\text{O}$, THF/MeOH ; (b) $\text{Na}_2\text{S} \cdot 9\text{H}_2\text{O}$, DMF.

The absorption spectra of porphyrin hybrid compounds are shown in Figure 4. Porphyrin-dipyrrin complex **3** shows a sharp Soret peak at 410 nm and weak peak at 530 nm, which is similar to the spectra addition of porphyrin and dipyrrin, indicating less electron transfer between porphyrin and dipyrrin unit. This phenomenon could be ascribed to the approximately vertical dihedral angle between two units in the crystal. Compared with **3**, por-bidipyrrin-por hybrid **4** presents a similar S band at 410 nm, shoulder peaks around 544 nm and a bathochromic-shift peak at 880 nm, which may be related to the conjugated bidipyrrin unit in the NIR component. Methoxy hybrid **6** shows a similar S bond with **4**, with a slight hypochromatic shifted Q bond at 860 nm. Porphyrin-dibromodipyrrin complex **7** shows an analogous spectrum to **3**, owing to their similar structures. In contrast to the open chain hybrids, compound **8** shows a subdued but broad S band at 410 nm, slightly red-shifted shoulder peaks at 540 nm and a broad Q band at 690 nm, which could be related to the thiacorrole unit.

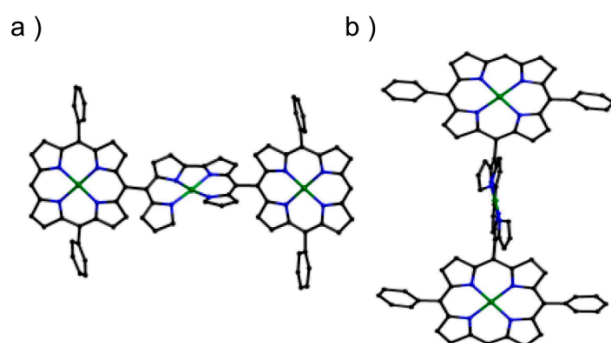


Figure 3. X-ray crystal structures of **4**. Solvent molecules, *tert*-butyl groups and hydrogen atoms were omitted for clarity (a) top view; (b) side view.

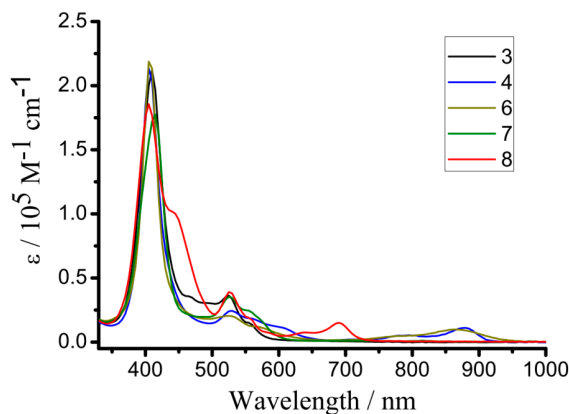


Figure 4. The absorption spectra of **3**, **4**, **6**, **7** and **8** in CH_2Cl_2 .

3. Materials and Synthesis

3.1. Materials and Instrumentation

All the reactions were performed in oven-dried reaction vessels under N_2 . Commercially available solvents and reagents were used without further purification unless otherwise mentioned. Thin-layer chromatography (TLC) was carried out on aluminum sheets coated with silica gel 60 F254 (MERCK, Darmstadt, Germany). ^1H -NMR spectra were obtained using a Bruker (Karlsruhe, Germany) AM 400 spectrometer, and chemical shifts were reported relative to CDCl_3 ($\delta = 7.26$) in ppm. ^{13}C -NMR spectra were recorded at 100 MHz (Bruker AM 400) and chemical shifts were reported relative to CDCl_3 ($\delta = 77.00$) in ppm. HRMS were performed using a Waters LCT Premier XE spectrometer (Milford, MA, USA). UV-Vis absorption spectra were recorded on a Varian

Cary 100 spectrophotometer and fluorescence spectra were recorded on a Varian Cary Eclipse (Anaheim, CA, USA) fluorescence spectrophotometer.

3.2. Crystallography

X-ray analyses were performed on a SMART APEX equipped with CCD detector (Bruker, Karlsruhe, Germany) using MoK α (graphite, monochromated, $\lambda = 0.71069 \text{ \AA}$) radiation and CuK α (graphite, monochromated, $\lambda = 1.54178 \text{ \AA}$) radiation. The structure was solved by the direct method of SHELXS-97 and refined using the SHELXL-97 program. The positional parameters and thermal parameters of non-hydrogen atoms were refined anisotropically on F^2 by the full-matrix least-squares method. Hydrogen atoms were placed at calculated positions and refined riding on their corresponding carbon atoms (Table 1). Single crystals of **3** and **4** were obtained by the slow recrystallization from solutions in dichloromethane/methanol.

Table 1. Crystallographic data and structure refinement summary for the compounds.

3	4
C ₁₁₄ H ₁₁₄ N ₁₂ Ni ₃	C ₁₁₄ H ₁₁₂ N ₁₂ Ni ₃
<i>Mr</i> = 1828.30	<i>Mr</i> = 1826.29
Orthorhombi	Triclinic
<i>C</i> 222(1)	<i>P</i> -1
<i>a</i> = 33.100(3)	<i>a</i> = 19.6380(18)
<i>b</i> = 24.600(2)	<i>b</i> = 20.1721(19)
<i>c</i> = 15.4400(14)	<i>c</i> = 27.330(3)
$\alpha = 90.00^\circ$	$\alpha = 73.257(2)^\circ$
$\beta = 90.00^\circ$	$\beta = 78.750(3)^\circ$
$\gamma = 90.00^\circ$	$\gamma = 67.5910(10)^\circ$
<i>V</i> = 12572.3(19) \AA^3	<i>V</i> = 9540.1(15) \AA^3
<i>Z</i> = 4	<i>Z</i> = 3
<i>R</i> ₁ = 0.1257	<i>R</i> ₁ = 0.1264
<i>wR</i> ₂ = 0.2693	<i>wR</i> ₂ = 0.2897
GOF = 1.038	GOF = 1.084

CCDC 1550953 (**3**) and 1550954 (**4**) contain the supplementary crystallographic data for this paper. These data can be obtained free of charge from The Cambridge Crystallographic Data Centre via www.ccdc.cam.ac.uk/data_request/cif.

3.3. Syntheses

3.3.1. Synthesis of **2**

Trifluoroacetic acid (0.25 mL, 2.6 mmol) was added to a solution of Ni^{II} (10,20-di(3,5-di-*tert*-butylphenyl))-5-formyl porphyrin (2.0 g, 2.6 mmol) and pyrrole (36 mL, 0.52 mol) and stirred for 2 h at room temperature under nitrogen. After neutralization with 1 N NaOH aq. (3.0 mL), the solution was extracted with CH₂Cl₂, dried over anhydrous Na₂SO₄ and evaporated in vacuo. Unreacted pyrrole was distilled under vacuum and the residue was purified by silica-gel column chromatography with a mixture of CH₂Cl₂ and *n*-hexane (*v/v* = 1/1) as an eluent. Recrystallization from CH₂Cl₂/MeOH gave red solid **2** (1.4 g, 65% yield).

¹H-NMR (400 MHz, CDCl₃) δ 9.71 (s, 1H), 9.20 (d, *J* = 5.2 Hz, 2H), 9.08 (d, *J* = 4.8 Hz, 2H), 8.88 (d, *J* = 4.8 Hz, 2H), 8.78 (d, *J* = 5.2 Hz, 2H), 8.11 (s, 2H), 7.83 (d, *J* = 1.8 Hz, 4H), 7.77 (s, 1H), 7.74 (t, *J* = 1.8 Hz, 2H), 6.62 (dd, *J* = 4.2, 2.6 Hz, 2H), 6.32 (d, *J* = 3.6 Hz, 2H), 6.24 (dd, *J* = 6.0, 2.8 Hz, 2H), 1.49 (s, 37H). ¹³C-NMR (100 MHz, CDCl₃) δ 149.05, 142.63, 142.33, 142.01, 141.74, 139.44, 135.16, 133.64, 132.93, 132.29, 130.27, 128.60, 121.26, 119.54, 116.99, 108.54, 107.34, 104.56, 43.45, 34.98, 31.67. HRMS [M + H]⁺ *m/z* = 887.4242, calcd. for C₅₇H₆₁N₆Ni = 887.4311.

3.3.2. Synthesis of 3

A solution of **2** (1.0 g, 1.12 mmol) in THF (250 mL) was treated with DDQ (280 mg, 1.24 mmol) at room temperature. After 50 min, 1 mL of Et₃N were added. A methanolic solution containing NiCl₂·6H₂O (2.0 g in 30 mL) was then added to the reaction mixture. The reaction proceeded for an additional 45 min, after which the TLC indicated no uncoordinated dipyrromethene. The reaction mixture was washed with water, dried over anhydrous Na₂SO₄ and evaporated in vacuo. The residue was purified by silica-gel column chromatography with CH₂Cl₂ as an eluent. Recrystallization from CH₂Cl₂/MeOH gave the deep red solid **3** (810 mg, 79% yield).

¹H-NMR (400 MHz, CDCl₃) δ 14.12 (s, 4H), 9.90 (s, 2H), 9.87 (s, 4H), 9.18 (d, *J* = 4.8 Hz, 4H), 8.98 (d, *J* = 4.8 Hz, 4H), 8.84 (dd, *J* = 11.8, 4.4 Hz, 8H), 7.96 (m, 8H), 7.80 (s, 4H), 6.24 (d, *J* = 2.8 Hz, 4H), 1.55 (s, 72H). ¹³C-NMR (100 MHz, CDCl₃) δ 150.00, 148.98, 143.41, 142.74, 142.51, 142.13, 139.88, 132.93, 132.66, 131.96, 128.84, 121.20, 120.29, 110.24, 105.52, 35.03, 31.71. HRMS [M + H]⁺ *m/z* = 1825.7453, calcd. for C₁₁₄H₁₁₄N₁₂Ni₃ = 1825.7428.

3.3.3. Synthesis of 4

A solution of **3** (1.1 g, 0.63 mmol) in toluene (150 mL) was treated with DDQ (0.21 g, 0.91 mmol) and heated at reflux for 12 h. After removal of the solvent, the residue was separated by silica gel column chromatography using CH₂Cl₂/hexane = 1/2 (*v/v*) to afford **4** as a deep brown solid (650 mg, 59% yield).

¹H-NMR (400 MHz, CDCl₃) δ 9.92 (s, 2H), 9.18 (dd, *J* = 6.0, 5.0 Hz, 8H), 8.96 (d, *J* = 4.8 Hz, 4H), 8.89 (d, *J* = 4.8 Hz, 4H), 7.94 (m, 8H), 7.78 (m, 4H), 6.50 (d, *J* = 4.4 Hz, 2H), 6.32 (s, 2H), 6.27 (s, 2H), 6.21 (s, 2H), 6.00 (d, *J* = 4.4 Hz, 2H), 1.52 (s, 72H). ¹³C-NMR (100 MHz, CDCl₃) δ 161.76, 153.19, 149.07, 144.82, 143.53, 143.28, 142.95, 142.64, 141.95, 140.97, 139.96, 133.11, 132.78, 132.22, 128.91, 121.31, 120.49, 116.16, 111.46, 105.59, 35.10, 31.79. HRMS [M + H]⁺ *m/z* = 1823.7160, calcd. for C₁₁₄H₁₁₃N₁₂Ni₃ = 1823.7272.

3.3.4. Synthesis of 5

A methanol solution (30 mL) of FeCl₃ (50 mg, 0.32 mmol) was added to a solution of **4** (110 mg, 0.06 mmol) in CH₂Cl₂ (100 mL). After stirring for 4 h, the reaction mixture was washed with water. The organic phase was dried over sodium sulfate, filtered, and concentrated under reduced pressure. The crude product (**5**) was used for the next reaction without purification.

3.3.5. Synthesis of 6

An ethanol (20 mL) solution of Ni(OAc)₂·2H₂O (100 mg, 0.44 mmol) was added to a toluene (70 mL) solution of **5** (110 mg, 0.06 mmol). The mixture was stirred at 70 °C for 4 h. After evaporation under vacuum, the residue was separated by silica gel column chromatography using CH₂Cl₂/hexane (1/2, *v/v*) to afford complex **6** (86 mg, 72%) as a dark red solid.

¹H-NMR (400 MHz, CDCl₃) δ 10.02 (d, *J* = 4.8 Hz, 2H), 9.87 (s, 2H), 9.19–9.13 (m, 4H), 9.09 (d, *J* = 4.8 Hz, 2H), 9.00–8.91 (m, 6H), 8.82 (d, *J* = 4.8 Hz, 2H), 7.92 (m, 12H), 5.87 (d, *J* = 4.0 Hz, 2H), 5.60 (d, *J* = 4.8 Hz, 2H), 5.44–5.32 (m, 4H), 3.68 (s, 6H), 1.57 (s, 72H). ¹³C-NMR (100 MHz, CDCl₃) δ 177.37, 150.50, 149.01, 143.57, 142.82, 142.47, 142.24, 140.53, 139.86, 138.03, 133.03, 132.58, 132.43, 131.64, 128.78, 127.84, 121.28, 120.05, 112.47, 111.31, 105.39, 103.84, 35.11, 31.81. HRMS [M + H]⁺ *m/z* = 1883.7591, calcd. for C₁₁₆H₁₁₇N₁₂Ni₃O₂ = 1883.7483.

3.3.6. Synthesis of 7

A solution of **2** (1.0 g, 1.12 mmol) in dry THF (250 mL) was cooled to −78 °C and NBS (400 mg, 2.24 mmol) and added in two portions over 1 h. A THF solution of DDQ (280 mg, 1.24 mmol) was added dropwise over 10 min. The reaction mixture was warmed to room temperature. After 50 min, 1 mL of Et₃N was added. A methanolic solution containing NiCl₂·6H₂O (2.0 g in 30 mL) was then added to the reaction mixture. The reaction proceeded for an additional 45 min. The reaction mixture

was washed with water, dried over anhydrous Na_2SO_4 , and evaporated in vacuo. The residue was purified by fast silica-gel column chromatography with CH_2Cl_2 as an eluent to give the deep red solid **7** (810 mg, 79% yield). The crude product was immediately used for the next reaction. HRMS $m/z = 2137.3844$, calcd. for $\text{C}_{114}\text{H}_{111}\text{Br}_4\text{N}_{12}\text{Ni}_3 = 2137.3849$.

3.3.7. Synthesis of **8**

A Schlenk tube containing **7** (122.2 mg, 50 mmol) and $\text{Na}_2\text{S}\cdot 9\text{H}_2\text{O}$ (24.0 mg, 0.10 mmol) was evacuated and then refilled with N_2 . Dry DMF (15 mL) was added, and mixture was stirred at 65°C for 5 h in oil bath. After cooling the reaction mixture to RT, the reaction mixture was washed with water, dried over anhydrous Na_2SO_4 , and evaporated in vacuo. The mixture was purified by silica-gel column chromatography (CH_2Cl_2 /hexane) to give **8** (12.6 mg, 20.7 mmol) in a 41% yield as black solid.

$^1\text{H-NMR}$ (400 MHz, CDCl_3) δ 10.00 (s, 2H), 9.25 (d, $J = 4.8$ Hz, 4H), 9.01 (d, $J = 4.7$ Hz, 4H), 8.75 (d, $J = 4.9$ Hz, 4H), 8.45 (d, $J = 4.9$ Hz, 4H), 8.35 (d, $J = 4.5$ Hz, 2H), 8.31 (d, $J = 4.7$ Hz, 2H), 7.97 (s, 8H), 7.87 (d, $J = 4.7$ Hz, 2H), 7.73 (t, $J = 1.7$ Hz, 4H), 7.63 (d, $J = 4.5$ Hz, 2H), 1.48 (s, 72H). $^{13}\text{C-NMR}$ (100 MHz, CDCl_3) δ 148.94, 145.47, 143.59, 142.74, 139.98, 139.51, 133.23, 132.71, 132.11, 130.72, 128.84, 121.65, 121.18, 120.76, 119.01, 105.50, 34.98, 31.66. HRMS $[\text{M} + \text{H}]^+ m/z = 1853.6588$, calcd. for $\text{C}_{114}\text{H}_{111}\text{N}_{12}\text{Ni}_3\text{S} = 1853.6836$.

4. Conclusions

In summary, we have successfully prepared a series of porphyrin hybrids with variously coordinated nickel metal. By oxidizing meso-Porphyrinyldipyrromethene **2** using DDQ in THF and subsequent coordination, por-dipyrin-por hybrid **3** was obtained in a high yield. The further oxidization of **3** afforded the por-bidipyrin-por hybrid **4**. Unexpectedly, treating **4** with FeCl_3 in CH_2Cl_2 /MeOH and subsequent coordination generated methoxy-substituted por-bidipyrin-por hybrid **6**. Fortunately, by treating dibromo por-dipyrin-por hybrid **7** with $\text{Na}_2\text{S}\cdot 9\text{H}_2\text{O}$, the expected por-thiacorrole-por hybrid **8** was successfully synthesized. In conclusion, meso-meso linked porphyrin hybrids play an important role in photoelectric or magnetic materials. Various linking methods were proven to be effective approaches for functional porphyrin materials. The further properties of these hybrids will be the main objective of our future work.

Supplementary Materials: Supplementary materials are available online.

Author Contributions: R.H. and J.K. conceived and designed the experiments; R.H. performed the experiments; H.Y. and J.K. analyzed the data; H.Y. contributed reagents/materials/analysis tools; J.H. wrote the paper.

Conflicts of Interest: The authors declare no conflict of interest.

References

1. Maruccio, G.; Cingolani, R.; Rinaldi, R. Projecting the nanoworld: Concepts, results and perspectives of molecular electronics. *J. Mater. Chem.* **2004**, *14*, 542–554. [[CrossRef](#)]
2. Fabian, J.; Nakazumi, H.; Matsuoka, M. Near-infrared absorbing dyes. *Chem. Rev.* **1992**, *92*, 1197–1226. [[CrossRef](#)]
3. Nalwa, H.S. Organic Materials for Third-Order Nonlinear Optics. *Adv. Mater.* **1993**, *5*, 341–358. [[CrossRef](#)]
4. Marrocchi, A.; Facchetti, A.; Lanari, D.; Petrucci, C.; Vaccaro, L. Current methodologies for a sustainable approach to π -conjugated organic semiconductors. *Energy Environ. Sci.* **2016**, *9*, 763–786. [[CrossRef](#)]
5. Ding, Y.B.; Tang, Y.Y.; Xie, Y.S. Fluorescent and colorimetric ion probes based on conjugated oligopyrroles. *Chem. Soc. Rev.* **2015**, *44*, 1101–1112. [[CrossRef](#)] [[PubMed](#)]
6. Ding, Y.B.; Zhu, W.H.; Xie, Y.S. Development of Ion Chemosensors Based on Porphyrin Analogues. *Chem. Rev.* **2017**, *177*, 2203–2256. [[CrossRef](#)] [[PubMed](#)]
7. Ding, Y.B.; Li, T.; Zhu, W.H. Highly selective colorimetric sensing of cyanide based on formation of dipyrin adducts. *Org. Biomol. Chem.* **2012**, *10*, 4201–4207. [[CrossRef](#)] [[PubMed](#)]

8. Ding, Y.B.; Xie, Y.S.; Li, X.; Hill, J.P.; Zhang, W.B.; Zhu, W.H. Selective and sensitive “turn-on” fluorescent Zn²⁺ sensors based on di- and tripyrrins with readily modulated emission wavelengths. *Chem. Commun.* **2011**, *47*, 5431–5433. [[CrossRef](#)] [[PubMed](#)]
9. Wang, Q.G.; Xie, Y.S.; Ding, Y.B.; Zhu, W.H. Colorimetric fluoride sensors based on deprotonation of pyrrole–hemiquinone compounds. *Chem. Commun.* **2010**, *46*, 3669–3671. [[CrossRef](#)] [[PubMed](#)]
10. Saito, S.; Osuka, A. Expanded porphyrins: Intriguing structures, electronic properties, and reactivities. *Angew. Chem. Int. Ed.* **2011**, *50*, 4342–4373. [[CrossRef](#)] [[PubMed](#)]
11. Stepien, M.; Sprutta, N.; Latos-Grazynski, L. Figure eights, Möbius bands, and more: Conformation and aromaticity of porphyrinoids. *Angew. Chem. Int. Ed.* **2011**, *50*, 4288–4340. [[CrossRef](#)] [[PubMed](#)]
12. Roznyatovskiy, V.V.; Lee, C.H.; Sessler, J.L. π -Extended isomeric and expanded porphyrins. *Chem. Soc. Rev.* **2013**, *42*, 1921–1933. [[CrossRef](#)] [[PubMed](#)]
13. Gill, H.S.; Finger, I.; Božidarević, S.F.; Scott, M.J. Preparation of α , β -unsubstituted meso-arylbidipyrins via metal-templated, oxidative coupling of dipyrins. *New J. Chem.* **2005**, *29*, 68–71. [[CrossRef](#)]
14. Hashimoto, T.; Nishimura, T.; Lim, J.M.; Kim, D.; Maeda, H. Formation of Metal-Assisted Stable Double Helices in Dimers of Cyclic Bis-Tetrapyrroles that Exhibit Spring-Like Motion. *Chem. Eur. J.* **2010**, *16*, 11653–11661. [[CrossRef](#)] [[PubMed](#)]
15. Ruffin, H.; Baudron, A.S.; Salazar-Mendoza, D.; Hosseini, W. A Silver Bite: Crystalline Heterometallic Architectures Based on Ag– π Interactions with a Bis-Dipyrin Zinc Helicate. *Chem. Eur. J.* **2014**, *20*, 2449–2453. [[CrossRef](#)] [[PubMed](#)]
16. Baudron, S.A.; Ruffin, H.; Hosseini, M.W. On Zn(ii) 2,2'-bisdipyrin circular helicates. *Chem. Commun.* **2015**, *51*, 5906–5909. [[CrossRef](#)] [[PubMed](#)]
17. Lakshmi, V.; Lee, W.-Z.; Ravikanth, M. Synthesis, structure and spectral and electrochemical properties of 3-pyrrolyl BODIPY-metal dipyrin complexes. *Dalton Trans.* **2014**, *43*, 16006–16014. [[CrossRef](#)] [[PubMed](#)]
18. Sakamoto, R.; Iwashima, T.; Tsuchiya, M.; Toyoda, R.; Matsuoka, R.; Kögel, J.F.; Kusaka, S.; Hoshiko, K.; Yagi, T.; Nagayama, T.; et al. New aspects in bis and tris(dipyrinato) metal complexes: Bright luminescence, self-assembled nanoarchitectures, and materials applications. *J. Mater. Chem. A* **2015**, *3*, 15357–15371. [[CrossRef](#)]
19. Gadekar, S.C.; Reddy, B.K.; Panchal, S.P.; Anand, V.G. Metal assisted cyclomerization of benzodipyrins into expanded norroles, aza-heptalene and acyclic dimmers. *Chem. Commun.* **2016**, *52*, 4565–4568. [[CrossRef](#)] [[PubMed](#)]
20. Lewtak, J.P.; Gryko, D.T. Synthesis of π -extended porphyrins via intramolecular oxidative coupling. *Chem. Commun.* **2012**, *48*, 10069–10086. [[CrossRef](#)] [[PubMed](#)]
21. Senge, M.O.; Fazekas, M.E.; Notaras, G.A.; Blau, W.J.; Zawadzka, M.; Locos, O.B.; Ni Mhuircheartaigh, E.M. Nonlinear optical properties of porphyrins. *Adv. Mater.* **2007**, *19*, 2737–2774. [[CrossRef](#)]
22. Pawlicki, M.; Collins, H.A.; Denning, R.G.; Anderson, H.L. Two-Photon Absorption and the Design of Two-Photon Dyes. *Angew. Chem. Int. Ed.* **2009**, *48*, 3244–3266. [[CrossRef](#)] [[PubMed](#)]
23. Davis, N.K.S.; Thompson, A.L.; Anderson, H.L. A Porphyrin Fused to Four Anthracenes. *J. Am. Chem. Soc.* **2011**, *133*, 30–31. [[CrossRef](#)] [[PubMed](#)]
24. Hoffmann, M.; Wilson, C.J.; Odell, B.; Anderson, P. Template-Directed Synthesis of a π -Conjugated Porphyrin Nanoring. *Angew. Chem. Int. Ed.* **2007**, *46*, 3122–3125. [[CrossRef](#)] [[PubMed](#)]
25. Nakamura, Y.; Jang, S.Y.; Tanaka, T.; Aratani, N.; Lim, J.M.; Kim, K.S.; Kim, D.; Osuka, A. Two-Dimensionally Extended Porphyrin Tapes: Synthesis and Shape-Dependent Two-Photon Absorption Properties. *Chem. Eur. J.* **2008**, *14*, 8279–8289. [[CrossRef](#)] [[PubMed](#)]
26. Nakamura, Y.; Aratani, N.; Shinokubo, H.; Takagi, A.; Kawai, T.; Matsumoto, T.; Yoon, Z.S.; Kim, D.Y.; Ahn, T.K.; Kim, D.; et al. A directly fused tetrameric porphyrin sheet and its anomalous electronic properties that arise from the planar cyclooctatetraene core. *J. Am. Chem. Soc.* **2006**, *128*, 4119–4127. [[CrossRef](#)] [[PubMed](#)]
27. Tanaka, T.; Lee, B.S.; Aratani, N.; Yoon, M.-C.; Kim, D.; Osuka, A. Synthesis and properties of hybrid porphyrin tapes. *Chem. Eur. J.* **2011**, *17*, 14400–14412. [[CrossRef](#)] [[PubMed](#)]
28. Mori, H.; Tanaka, T.; Lee, B.S.; Kim, P.; Kim, D.; Osuka, A. An Electron-Deficient Porphyrin Tape. *Chem. Asian J.* **2012**, *7*, 1811–1816. [[CrossRef](#)] [[PubMed](#)]

29. Bonifazi, D.; Scholl, M.; Song, F.Y.; Echegoyen, L.E.; Accorsi, G.; Armaroli, N.; Diederich, F. Exceptional redox and photophysical properties of a triply fused diporphyrin- C_{60} conjugate: Novel scaffolds for multicharge storage in molecular scale electronics. *Angew. Chem. Int. Ed.* **2003**, *115*, 5116–5120. [[CrossRef](#)]
30. Kim, D.; Osuka, A. Directly linked porphyrin arrays with tunable excitonic interactions. *Acc. Chem. Res.* **2004**, *37*, 735–745. [[CrossRef](#)] [[PubMed](#)]
31. Aratani, N.; Kim, D.; Osuka, A. π -Conjugation Enlargement toward the Creation of Multi-Porphyrinic Systems with Large Two-Photon Absorption Properties. *Chem. Asian J.* **2009**, *4*, 1172–1182. [[CrossRef](#)] [[PubMed](#)]
32. Mori, H.; Tanaka, T.; Osuka, A. Fused porphyrinoids as promising near-infrared absorbing dyes. *J. Mater. Chem. C* **2013**, *1*, 2500–2519. [[CrossRef](#)]
33. Tanaka, T.; Osuka, A. Conjugated porphyrin arrays: Synthesis, properties and applications for functional materials. *Chem. Soc. Rev.* **2015**, *44*, 943–969. [[CrossRef](#)] [[PubMed](#)]
34. Davis, N.K.S.; Thompson, A.L.; Anderson, H.L. Bis-anthracene fused porphyrins: Synthesis, crystal structure, and near-IR absorption. *Org. Lett.* **2010**, *12*, 2124–2127. [[CrossRef](#)] [[PubMed](#)]
35. Lindsey, J.S.; Prathapan, S.; Johnson, T.E.; Wagner, R.W. Porphyrin building blocks for modular construction of bioorganic model systems. *Tetrahedron* **1994**, *50*, 8941–8968. [[CrossRef](#)]
36. Maruyama, K.; Kawabata, S. Synthesis and characterization of polyene porphyrins. *Bull. Chem. Soc. Jpn.* **1990**, *63*, 170–175. [[CrossRef](#)]
37. Tsuda, A.; Osuka, A. Fully conjugated porphyrin tapes with electronic absorption bands that reach into infrared. *Science* **2001**, *293*, 79–82. [[CrossRef](#)] [[PubMed](#)]
38. Chen, C.; Zhu, Y.-Z.; Fan, Q.-J.; Song, H.-B.; Zheng, J.-Y. Crystal Structure, and Spectroscopic Properties of Meso-Meso-Linked Porphyrin-Corrole Hybrids. *Chem. Lett.* **2013**, *42*, 936–938. [[CrossRef](#)]
39. Murugavel, M.; Reddy, R.; Sankar, J. A new meso-meso directly-linked corrole-porphyrin-corrole hybrid: Synthesis and photophysical properties. *RSC Adv.* **2014**, *4*, 13669–13672. [[CrossRef](#)]
40. Mori, H.; Tanaka, T.; Lee, S.; Osuka, A.; Lim, J.M.; Kim, D.; Osuka, A. meso-meso Linked Porphyrin-[26]Hexaphyrin-Porphyrin Hybrid Arrays and Their Triply Linked Tapes Exhibiting Strong Absorption Bands in the NIR Region. *J. Am. Chem. Soc.* **2015**, *137*, 2097–2106. [[CrossRef](#)] [[PubMed](#)]
41. Tanaka, T.; Aratani, N.; Lim, J.M.; Osuka, A.; Kim, K.S.; Kim, D.; Osuka, A. Porphyrin-hexaphyrin hybrid tapes. *Chem. Sci.* **2011**, *2*, 1414–1418. [[CrossRef](#)]
42. Li, F.R.; Yang, S.I.; Ciringh, Y.Z.; Seth, J.; Martin, C.H.; Singh, D.L.; Kim, D.; Birge, R.R.; Bocian, D.F.; Holten, D.; et al. Design, synthesis, and photodynamics of light-harvesting arrays comprised of a porphyrin and one, two, or eight boron-dipyrin accessory pigments. *J. Am. Chem. Soc.* **1998**, *120*, 10001–10007. [[CrossRef](#)]
43. Lee, C.Y.; Jang, J.K.; Kim, C.H.; Jung, J.; Park, B.K.; Park, J.; Choi, W.; Han, Y.K.; Joo, T.; Park, J.T.; et al. Remarkably efficient photocurrent generation based on a [60]fullerene-triosmium cluster/Zn-porphyrin/boron-dipyrin triad SAM. *Chem. Eur. J.* **2010**, *16*, 5586–5599. [[CrossRef](#)] [[PubMed](#)]
44. Kamiya, H.; Kondo, T.; Sakida, T.; Yamaguchi, S.; Shinokubo, H. meso-Thiaporphyrinoids Revisited: Missing of Sulfur by Small Metals. *Chem. Eur. J.* **2012**, *18*, 16129–16135. [[CrossRef](#)] [[PubMed](#)]

Sample Availability: Samples of the compounds are not available from the authors



© 2017 by the authors. Licensee MDPI, Basel, Switzerland. This article is an open access article distributed under the terms and conditions of the Creative Commons Attribution (CC BY) license (<http://creativecommons.org/licenses/by/4.0/>).